

Influence of Cultivation Conditions on Spatial Structure and Functional Activity of OmpF-Like Porin from Outer Membrane of *Yersinia pseudotuberculosis*

O. D. Novikova¹, T. I. Vakorina^{1*}, V. A. Khomenko¹, G. N. Likhatskaya¹, N. Yu. Kim¹,
V. I. Emelyanenko², S. M. Kuznetsova², and T. F. Solov'eva¹

¹Pacific Institute of Bioorganic Chemistry, Far East Branch, Russian Academy of Sciences, pr. 100 let Vladivostoku 159, 690022 Vladivostok, Russia; fax: (4232) 314-050; E-mail: vakorina@piboc.dvo.ru

²Institute of Theoretical and Experimental Biophysics, Russian Academy of Sciences, 142292 Pushchino, Moscow Region, Russia

Received June 26, 2007

Revision received July 28, 2007

Abstract—The influence of cultivation conditions of pseudotuberculosis bacteria on the spatial structure and the functional activity of nonspecific OmpF-like porin was studied by means of optical spectroscopy, scanning microcalorimetry, and bilayer lipid membrane technique. With this goal, porin samples isolated from microbial masses grown at different temperatures, nutrient medium densities, and growth phases were characterized. According to CD data, the porin samples under investigation represent β -sheet proteins. It was found that the protein isolated from the colonial culture of pseudotuberculosis bacteria grown at low temperature has the most compact structure. Using intrinsic protein fluorescence, it was shown that different conditions of pseudotuberculosis bacteria cultivation (temperature, medium, growth phase) led to the changes in spectral properties of porin fluorescence due to the redistribution of the contributions of tyrosine and different classes of tryptophan residues to the total protein emission. Heat inactivation of porin samples was studied using CD spectroscopy, intrinsic protein fluorescence, and scanning microcalorimetry. Spatial features of the porin samples were found to affect their functional activities. Considering all these data, it is possible to correlate the spatial structure and functional activity of porin samples isolated under different cultivation conditions of bacteria and the composition of the outer membrane lipid matrix.

DOI: 10.1134/S0006297908020041

Key words: nonspecific OmpF-like porins, spatial structure, thermostability, functional activity, lipid matrix

The cell membrane lipids play an important role in protein biosynthesis. Recently a number of papers have been published on the influence of lipid composition of the membrane on the structure and properties of its components, including porins [1, 2]. Here it is well known the functionally active lipids in the outer membrane (OM) of gram-negative bacteria play a defining role for the folding and insertion of these integral proteins as well as for their pore-forming activity [3, 4]. Along with other compo-

nents of bacterial OM, porins participate in the microorganisms' adaptation to different environmental conditions. It is known [5, 6] that alterations in membrane permeability caused by conformational plasticity of porins and/or expression of proteins with different pore diameter represent the one of the pathways of bacterial adaptation to varying growth conditions [5].

In nature, bacteria usually grow on a solid surface in the form of aggregates, colonies, and films, and this non-homogenous growth is significantly more variable and complicated compared to the homogenous one characteristic for liquid media [7]. The bacteria of *Yersinia pseudotuberculosis* are widely spread in the environment and adapted to grow in suspension (suspension culture) as well as on solid substrates in the form of colonies (colonial culture). The epidemiologically most important properties of the pseudotuberculosis microorganism are

Abbreviations: BLM) bilayer lipid membrane; DPG) diphosphatidylglycerol; LPE) lysophosphatidylethanolamine; LPh) logarithmic growth phase; NA) nutrient agar; NB) nutrient broth; NL) neutral lipids; OM) bacterial outer membrane; PE) phosphatidylethanolamine; PG) phosphatidylglycerol; PGPC) peptidoglycan–protein complexes; SPh) early stationary growth phase.

* To whom correspondence should be addressed.

its stability to various environmental conditions and ability to grow at low temperatures [8, 9]. Differences in the biological properties of *Yersinia* are to high extent connected to the efficiency of bacterial OM permeability. The latter is defined by OM composition and structure. The structure of OM is determined not only by temperature, but also by other cultivation conditions, i.e. medium density and bacteria growth phase [10, 11].

Earlier we showed [12] that the qualitative composition of phospholipids and fatty acids of pseudotuberculosis bacteria only slightly depends upon cultivation approach. However, the quantity of free lipids and relative content of phospholipids and neutral lipids (NL) in lipid extracts of *Y. pseudotuberculosis* varied with culture age and growth medium used (on nutrient broth (NB) or nutrient agar (NA)) [12]. Phospholipid content changed and the character of its alteration during cell aging showed different tendencies for suspension and colonial cultures. The bacteria had significantly higher content of phospholipids in stationary phase when grown on NA compared to that during growth on NB (2.6 and 1.7%, respectively). This tendency was clearest for changes in the lysophosphatidylethanolamine (LPE) content. Adherent bacteria in linear and early stationary phase had an anomaly high level of LPE (35.9 and 18.2%, respectively) compared to free living microorganisms (6.1 and 5.5%, respectively) [12].

Determination of structural features and elucidation of modulation mechanisms of functionally active porins in OM of gram-negative bacteria draw great interest. The aim of the present work was to study the influence of pseudotuberculosis bacteria cultivation conditions (and its OM lipid matrix composition, accordingly) on the structural organization and functional activity of OmpF-like nonspecific porin from *Y. pseudotuberculosis* OM (yersinin).

Gel electrophoresis in presence of SDS (SDS-PAGE), optical spectroscopy (intrinsic protein fluorescence and CD), and scanning microcalorimetry were used to investigate the structural features of the protein. Pore-forming properties of the yersinin samples in peptidoglycan-protein complexes (PGPC) were studied using bilayer lipid membrane (BLM). We used this approach earlier [13] for comparative study of pore-forming proteins in OM of pathogenic and nonpathogenic *Yersinia*. Porins maintain their native environment in the above-mentioned complexes. Therefore, using PGPC reconstruction it is possible to determine the differences in functional activity of the studied proteins, which are evened during solubilization of bacterial OM.

MATERIALS AND METHODS

Bacterial cultivation. Strain H-557 of *Y. pseudotuberculosis* of serotype 0:1B was used in the present work. The

bacteria were cultivated at 4°C ("cold" variant, C) (yersinin samples 1-3) and at 37°C ("warm" variant, W) (sample 4). Samples 1 and 2 were grown at 4°C on a solid substrate (NA) during four and seven days, respectively, which corresponds to logarithmic (LPh) and early stationary (SPh) growth phases. Sample 3 of *Y. pseudotuberculosis* contained yersinin from the "cold" variant of pseudotuberculosis bacteria grown on NB (Makhachkala, Russia) in 1-liter flasks with intensive aeration for five days (stationary growth phase in these conditions). Sample 4 represents yersinin isolated from "warm" pseudotuberculosis bacteria grown on NA/NB for 3/1.5 days, respectively (*Y. pseudotuberculosis* stationary growth phase in these conditions).

After achieving appropriate age, bacterial cultures were killed with 1% phenol solution for 20 min and separated from the culture medium by centrifugation at 5000 rpm for 20 min. Then the pellet was washed twice with isotonic solution using centrifugation under the same conditions.

Isolation of pore-forming protein fractions. Samples of bacterial mass were treated with Triton X-100 selectively extracting cytoplasmic membrane components [14]. Then PGPC were prepared using extraction with 2% SDS at 37°C as described in [13]. Pure porins were isolated according to Nurminen [15] by treating the peptidoglycan layer with lysozyme.

Purification of porin trimers. Yersinin was purified using gel filtration on Toyopearl HW-60F (TSK-gel; Toyo Soda, Japan) in 5 mM phosphate buffer, pH 7.8, containing 0.25% SDS (buffer A) as described previously [16]. The degree of purity of porin samples obtained was analyzed by means of SDS-PAGE [17] without heat treatment of samples or after boiling them for 5 min. Proteins in the gel were stained with Coomassie Blue G-250 solution in 3.5% perchloric acid [18], and the presence of lipopolysaccharide was identified upon staining gels with silver ions [19]. Monosaccharide content in protein samples was determined by a standard method [20]. A modified Lowry method in the presence of 2% SDS [21] was used to determine protein concentration in preparations. Porin preparations contained 85-90% protein and less than 5% monosaccharides.

UV-spectra were registered at 25°C on a Cecil CE 7200 spectrophotometer (Aquarus, Great Britain) in quartz cuvettes with optical path length of 1 cm. Protein concentration was determined in buffer A using absorbance maximum of UV spectra at 280 nm and $A_{1\text{ cm}}^{1\%}$ equal to 1.27 (the extinction coefficient of porin was determined experimentally).

CD spectra were registered on Jasco-500A spectropolarimeter (Jasco, Japan) in quartz cuvettes with optical path length of 0.1 cm for peptide and 1 cm for aromatic regions of the spectrum. The cuvette with protein solution in buffer A was thermostatted at given temperature for 20-25 min before registering the CD spectrum.

Additional registration of the spectrum at the same temperature showed its full coincidence with the previously recorded one. The accuracy of temperature measurements was $\pm 0.5^\circ\text{C}$. To exclude solvent evaporation at high temperatures, protein solution in the cuvette was covered with a layer of vaseline oil. In the peptide region of the CD spectrum (190–230 nm) ellipticity ($[\theta]$, $\text{deg}\cdot\text{cm}^2\cdot\text{dmol}^{-1}$) was calculated as ellipticity of amino acid residue assuming an average molecular weight as 110 daltons:

$$[\theta] = [\theta]_{\text{obs}} \cdot S \cdot 110 / 10 \cdot C \cdot l,$$

where S is sensitivity of the instrument scale, C is weight concentration of the protein (mg/ml), l is optical path length (mm). In the aromatic region of the CD spectra (240–320 nm) ellipticity was calculated as a molar ellipticity $[\theta]_M$ of porin in oligomeric form with the molecular weight of 110 kD. The spectropolarimeter was calibrated using 0.06% aqueous solution of ammonium salt of 10-sulfonate-D-camphoric acid (Katayama Chemical, Japan). The band ellipticity ratio at 192 and 290 nm was 2.09. The calculations of secondary structure elements were performed according to the Provencher–Glockner method [22].

Fluorescence spectra were measured on automated lab-made spectrofluorimeter with excitation from a mercury lamp (280.4 nm) and fluorescent light collection from the front surface of the cuvette. Spectral width of monochromator slots did not exceed 2 nm. Fluorescence spectra were corrected for the spectral sensitivity of the instrument [23]. When porin thermostability was studied, protein solution in buffer A was heated using a Peltier thermoelement mounted in the cuvette holder. Temperature in cuvette was measured using a thermocouple. Deconvolution of experimental spectra into components corresponding to tyrosine residue emission and spectral forms of tryptophan residues in the protein [24] were performed using an optimization program based on the Marquardt method [25].

Microcalorimetry study. Temperature dependence of excess specific heat capacity of porin solutions in buffer A was registered with a DASM-4 differential adiabatic microcalorimeter (Russian Academy of Sciences, Pushchino, Russia). All measurements were performed at heating velocity of $1^\circ\text{C}/\text{min}$. The thermally-induced transition temperatures (at given scanning velocity) were determined at the maximum point of temperature dependence of excess heat capacity.

Pore-forming activity. The instrument description and the protocol of electric parameter measurements in BLM are described in [26]. The BLM was formed according to the method of Muller from solution of 1-monooleoylglycerol in *n*-heptane as described in [26]. The aqueous phase contained 100 mM NaCl in buffer A and isolated yersinin trimers (protein concentration

0.01 $\mu\text{g}/\text{ml}$) or PGPC solubilized in 2% SDS (protein concentration 0.01–5 $\mu\text{g}/\text{ml}$). Protein concentration in PGPC was calculated assuming that the main pore-forming protein content in a fraction of proteins associated with peptidoglycan was not higher than 40% [13].

RESULTS AND DISCUSSION

Basis for porin sample choice. To obtain pseudotuberculosis bacteria with different phospholipid composition, we used the above-described features of *Y. pseudotuberculosis* to change phospholipid content of OM under the influence of cultivation conditions, especially medium density, phase, and temperature of growth. This approach allowed us to use the same microorganism strain for obtaining four variants of bacterial cells different in phospholipid composition and lipopolysaccharide structure (particularly, the length of O-specific polysaccharide chains), and for isolating four porin samples, accordingly. Table 1 shows that the main differences in membrane phospholipid composition are the ratio of the content LPE and zwitterionic phosphatidylethanolamine (PE) to sum of acidic phospholipids (phosphatidylglycerol (PG) and diphosphatidylglycerol (DPG)).

Therefore, in this study we compared the spatial organization and functional activities of porins grown at 4°C in different medium (NA or NB) and, in the case of colonial pseudotuberculosis bacterial culture, at different growth phase. Also, yersinin samples isolated from *Y. pseudotuberculosis* cells grown at 37°C in NA or NB and collected at stationary growth phase was used in the present work to evaluate the influence of cultivation temperature on the structure and pore-forming properties of yersinin. As demonstrated from the preliminary data, the medium density was not important for the “warm” variant of pseudotuberculosis bacteria.

Isolation of pore-forming proteins. We used a method of Nurmenen [15] to isolate pore-forming proteins. The method is based on porin stability to treatment with pro-

Table 1. Characterization of phospholipid composition of pseudotuberculosis bacterial OM porin samples

Sample	Degree of polymerization (<i>n</i>) of O-specific polysaccharide	Phospholipid content, %	
		LPE	PE/(PG + DPG)
1	4.0	8.4	1.6
2	12.0	35.9	4.3
3	4.0	5.5	1.9
4	2.0	not determined	

teolytic enzymes, in particular to trypsin. The method involves destruction of the bacterial peptidoglycan layer with lysozyme, incubation of cell envelopes with trypsin in presence of nonionic detergent Triton X-100 to remove satellite proteins [14], and 0.5 M NaCl precipitation of porin oligomers from the solution at pH 6.0 and 42°C. Further purification of the porins was achieved by gel filtration on Sephacryl S-300 in presence of SDS. According to SDS-PAGE data, all the porin samples isolated from bacteria cultivated under different conditions (samples 1-4) were in oligomeric form in presence of SDS and had molecular weights of 105-120 kD (data not shown). The proteins were heat-modifiable and transformed to heat-modified (denatured) form with apparent molecular mass of around 40 kD upon heating to 100°C in presence of 2% SDS. SDS-PAGE staining with silver ions [19] revealed the presence of the lipopolysaccharide in all samples.

Comparative study of spatial structure of porin samples from pseudotuberculosis bacteria cultivated under different conditions. *UV spectroscopy.* UV absorption spectra of "cold" variant porin solutions (samples 1, 2, and 3) are typical protein spectra with maximum around 280 nm and minimum at 250 nm. The UV spectra of these porin samples had distinct shoulder at 290 nm pointing to a substantial number of tryptophan residues in the protein. The UV spectrum of "warm" porin variant (sample 4) had the

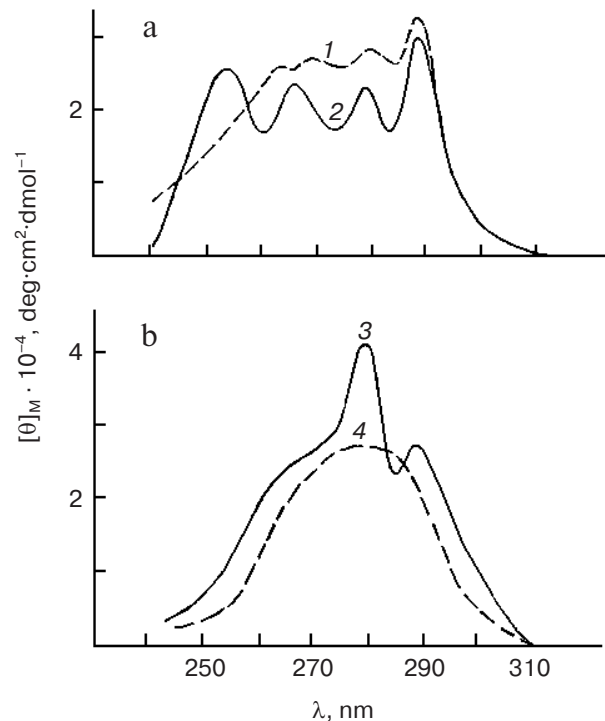


Fig. 1. CD spectra of porins in the near UV-region; $t = 25^{\circ}\text{C}$, pH 7.2. a: 1, 2) samples 1 (C-LPh-NA) and 2 (C-SPh-NA), respectively. b: 3, 4) samples 3 (C-SPh-NB) and 4 (W-SPh-NA/NB), respectively. Protein concentration, 290-450 $\mu\text{g/ml}$.

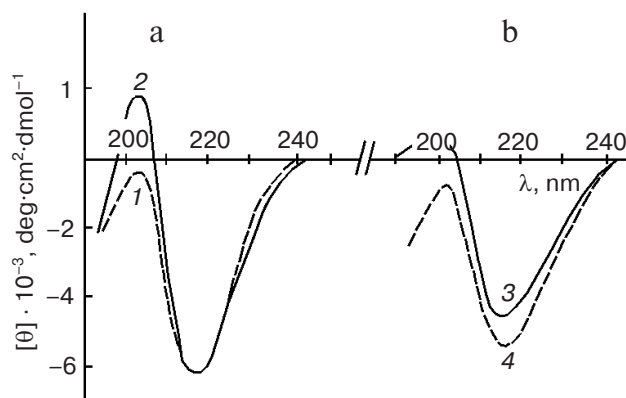


Fig. 2. CD spectra of porins in the far UV-region; $t = 25^{\circ}\text{C}$, pH 7.2. a: 1, 2) samples 1 (C-LPh-NA) and 2 (C-SPh-NA), respectively. b: 3, 4) samples 3 (C-SPh-NB) and 4 (W-SPh-NA/NB), respectively. Protein concentration, 120-200 $\mu\text{g/ml}$.

shape of a denatured protein—a curve with a maximum at 280 nm, as for other porin samples, but without a marked minimum at 250 nm (spectra not shown).

Circular dichroism. The CD spectra of "cold" variant porins (samples 1, 2, and 3) in the near UV region (240-320 nm)—the absorbance region of aromatic chromophore residues and disulfide bonds—had positive bands at 290 nm (tryptophan residues) and 280 and 268 nm (tyrosine/phenylalanine residues) (Fig. 1, a and b). The CD spectrum of sample 2 had more fine structure in this region compared to other porins (Fig. 1a). This points at an asymmetric environment of side-chain groups of these aromatic amino acid residues, their rigid fixation, and highly organized tertiary structure of this protein.

The "warm" variant porin CD spectra (sample 4) in near UV region (Fig. 1b) showed a smooth concave-downwards curve pointing to the absence of pronounced tertiary structure of porin 4. The reason for this could be looser structure of this protein or a presence of a mixture of closely related proteins with different conformations in the solution of porin from the "warm" variant bacteria.

The CD spectra of the porin samples in far UV (190-240 nm)—the region of peptide bond absorbance—were similar except for sample 2 (Fig. 2, a and b). All spectra had a negative minimum at 215-217 nm, and spectra of samples 1 and 4 had a negative maximum at 204 nm. The spectra of samples 2 and 3 had a positive band at 203 and 200 nm, respectively, and the intensities of these bands were substantially different (Fig. 2, a and b).

The secondary structure element content of porins was calculated according to Provencher and Glockner [22] based on the CD spectral data in the far UV region. The results are presented in Table 2. It shows that all of the porin samples were proteins whose secondary structure is mostly regular β -sheets. Its content in sample 2 was somewhat higher than that in the other porin samples.

Table 2. Secondary structure element content in porins from pseudotuberculosis bacteria grown under different conditions

Sample	α -Helix	β -Sheet	β -Turn	Random coil
1	0.0	0.55	0.06	0.39
2	0.0	0.62	0.04	0.34
3	0.0	0.59	0.08	0.30
4	0.0	0.52	0.18	0.30

It should be noted that porin sample 4 had 2-4-fold more β -turn in its secondary structure than samples 1, 2, and 3 (Table 2). This could indicate that this protein isolated from pseudotuberculosis bacteria grown at higher temperature is more unstable. Some data [27] indicate that structural stability of β -turns depends on the conformation of segments connecting them. For example, it was found that during conformational change in prion proteins a conformation rich in β -turns precedes the formation of their fibrillary neurotoxic form [28].

Intrinsic protein fluorescence. This method was used to elucidate tertiary structural features of the environment of aromatic fluorophores in the porin samples. Figure 3 shows the spectra of total protein fluorescence of samples obtained from bacteria cultivated under different conditions. Figure 3 shows that alteration of cultivation conditions substantially affected the form and position of maximum of fluorescence spectra determined by the microenvironment of the aromatic fluorophores of the porins. The fluorescence spectral maximum for protein samples 1 and 2 from "cold" variant of cells grown on solid substrate is positioned in the short-wavelength region of the spectrum at 320 nm. This indicates a large contribution in protein emission of tyrosine residues and tryptophan residues of classes S and I located in more hydrophobic environment in comparison with tryptophan residues class III. The shift of emission maximum to longer wavelength in the UV region of the spectrum ($\lambda_{\max} = 330$ nm) was observed for sample 3 isolated from the "cold" variant of bacterial suspension culture. Finally, an increase in cultivation temperature leads to dramatic spectral change: the long-wavelength position of the total fluorescence maximum of sample 4 porin ($\lambda_{\max} = 338$ nm) argues for high contribution of fluorophores accessible to water.

The dashed line in Fig. 3 represents the fluorescence spectra of tyrosine and discrete classes of tryptophan residues that contribute to the emission spectra of sample 3. The relative contributions of tyrosine residues and tryptophan spectral classes in the emission of all of the porin samples are presented in Table 3.

Table 3 shows that the greatest contribution to the spectrum of porin isolated from "warm" pseudotuberculosis bacteria (sample 4) is caused by the emission of class III tryptophan residues with λ_{\max} of 350-353 nm, corre-

sponding to the emission of free tryptophan. Tryptophan residues of S ($\lambda_{\max} = 316$ -317 nm) and I classes ($\lambda_{\max} = 330$ -332 nm) whose emission is defined by their location inside the protein molecule and by hydrophobic environment masking fluorophores from the solvent contributed least in the fluorescence spectra of this sample.

The content and ratio of contributions of two tryptophan residue classes (S and III) in proteins isolated from the "cold" variant of colonial cell culture during LPh and SPh (samples 1 and 2) are very similar. These proteins differ only in the contribution of class I tryptophan residues ($\lambda_{\max} = 330$ nm). The spectrum of porin isolated from "cold" suspension culture (sample 3) differed from spectra of samples 1 and 2 in lower contribution of tyrosine residues and higher input from tryptophan type III residues, apparently due to a lower content of S-type of these fluorophores (Table 3). This suggests that changing of any one cultivation parameter leads to an alteration both in microenvironment of tryptophan residues and in interpositions of tyrosines and tryptophans.

Therefore, spatial organization of porin molecule on the level of tertiary structure appeared to be sensitive to the alteration of cultivation conditions, which as men-

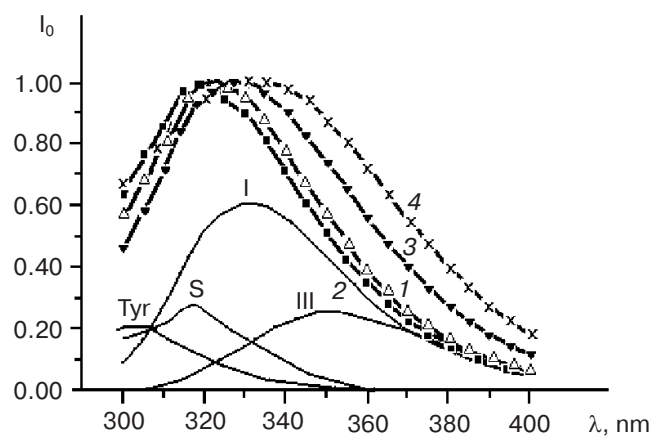


Fig. 3. Total fluorescence spectra of porin samples isolated from bacteria cultivated under different conditions: 1) sample 1 (C-LPh-NA); 2) sample 2 (C-SPh-NA); 3) sample 3 (C-SPh-NB); 4) sample 4 (W-SPh-NA/NB). Dashed lines show the contribution of tyrosine residues (Tyr) and tryptophan spectral forms (S, I, III) for sample 3. Protein concentration, 70-100 μ g/ml.

Table 3. Contribution of tryptophan spectral forms to the total emission of different porin samples

Sample	Tyrosine	Tryptophan forms				Transition temperature, °C		
		S	I	II	III	*	**	***
1	0.19	0.22	0.48	0	0.11		69	72
2	0.23	0.26	0.39	0	0.12	74	71	75
3	0.13	0.14	0.40	0	0.33	76	75	77
4	0.25	0.04	0.22	0	0.49	70	62	68

* Determined from microcalorimetry data.

** Determined from intrinsic fluorescence data.

*** Determined from CD spectra.

tioned above caused specific changes in lipid content and accordingly in the composition and properties of bacterial OM.

Analysis of modifications in porin spatial structure with temperature. In the next step of our work we determined the temperature transition point for the porin samples and analyzed changes in spatial organization of the protein molecule on the level of tertiary and secondary structure by means of optical spectroscopy and scanning microcalorimetry (Figs. 4–7).

Circular dichroism. The character of changes in secondary structure of porin samples 1, 2, and 4 during heating is similar. Nevertheless, the analysis of CD spectra of the protein samples at 85°C shows differences in degree of these changes. CD spectra of samples 2 and 4 at different temperatures are showed in Fig. 4 as examples. CD spectra of samples 1 and 3 are not showed because the course of temperature curves for samples 1 and 4 is similar, and changes in secondary structure of sample 3 are minimal.

Heating of a solution of sample 2 (isolated from “cold” variant of colonial cell culture during SPh growth phase) to 50°C does not lead to any changes in the CD spectrum. When increasing solution temperature to 60°C slight reduction of ellipticity of bands at 217 and 203 nm was observed in the CD spectrum (spectrum not shown). Further increase in the temperature of a solution of this protein led to shift of a negative minimum of the spectrum to shorter wavelength and appearance of a negative maximum at 199 nm (Fig. 4a). The form of this porin CD spectrum at 85°C assumes the appearance of α -helix in its secondary structure. During temperature denaturation of porin sample 3, a slight reduction of ellipticity of negative band and its “expansion” by 10–15 nm towards shorter wavelengths takes place only at 85°C. During heating of sample 4 to 70°C, reduction of ellipticity of minimum and of maximum of the negative band is observed in the CD spectra, while sharp increase in ellipticity of minimum of the negative band with its shift towards shorter wavelengths occurs at 85°C (Fig. 4b).

To estimate the thermostability of the studied proteins the conformational transition point at the level of

secondary structure was determined from the dependence of ellipticity at 222 nm on temperature. During protein denaturation studies the ellipticity changes at given wavelength is used as a degree of order of protein secondary structure [29].

Conformational transitions points for samples 1, 2, 3, and 4 occurred at 72, 75, 77, and 68°C, respectively. Therefore, the secondary structure of porin from “warm” bacterial variant (sample 4) was the most thermally unstable, while the most thermally stable porin was sample 3 protein isolated from “cold” suspension cell culture collected during SPh growth phase. Conformational changes in secondary structure of all the proteins under investigation were irreversible at temperatures higher than the corresponding transition temperatures.

Thermal denaturation of secondary structure of porin 2 isolated from “cold” colonial cell culture collected at SPh growth phase goes through an isodichroic point at 211 nm (Fig. 4a). The CD spectra of the other protein samples did not contain this point (Fig. 4b). Thermal denaturation of porin 4 is presented as an example. The presence of the isodichroic point means that porin transition from native to denatured state is a one-step cooperative process [30]. At the initial (25°C) and final (85°C) solution temperatures, the protein exists in only two spectrally different states having conformations of native and denatured protein, respectively. Under these conditions, this protein solution does not contain significant quantities of any partially degraded intermediate states (intermediates). Therefore, the CD spectrum recorded at an intermediate temperature is a linear combination of CD spectra of the protein in native and denatured states.

The absence of an isodichroic point in the CD spectra in the peptide region during heat denaturation of porin samples 1, 3, and 4 indicated that in these cases the protein solutions contain porin intermediates together with the main forms of the protein. It will be elucidated in the further studies whether these porin conformational states result from heat denaturation or are an attribute of the initial protein state in bacterial OM. Anyway, this shows that the alteration of bacterial cultivation condi-

tions leads to certain changes in spatial organization of the porin molecule favoring the conformational plasticity of these proteins.

Scanning microcalorimetry. Using scanning microcalorimetry we determined melting points of porin samples 2, 3, and 4 (Fig. 5). Analysis of the thermograms suggests the following conclusions. The change in the cultivation medium has virtually no effect of thermostability of the protein—maxima of the melting curves of samples 2 and 3 were at 74 and 76°C, respectively (Table 2). At the same time, increase in pseudotuberculosis bacteria growth temperature decreases the thermal transition

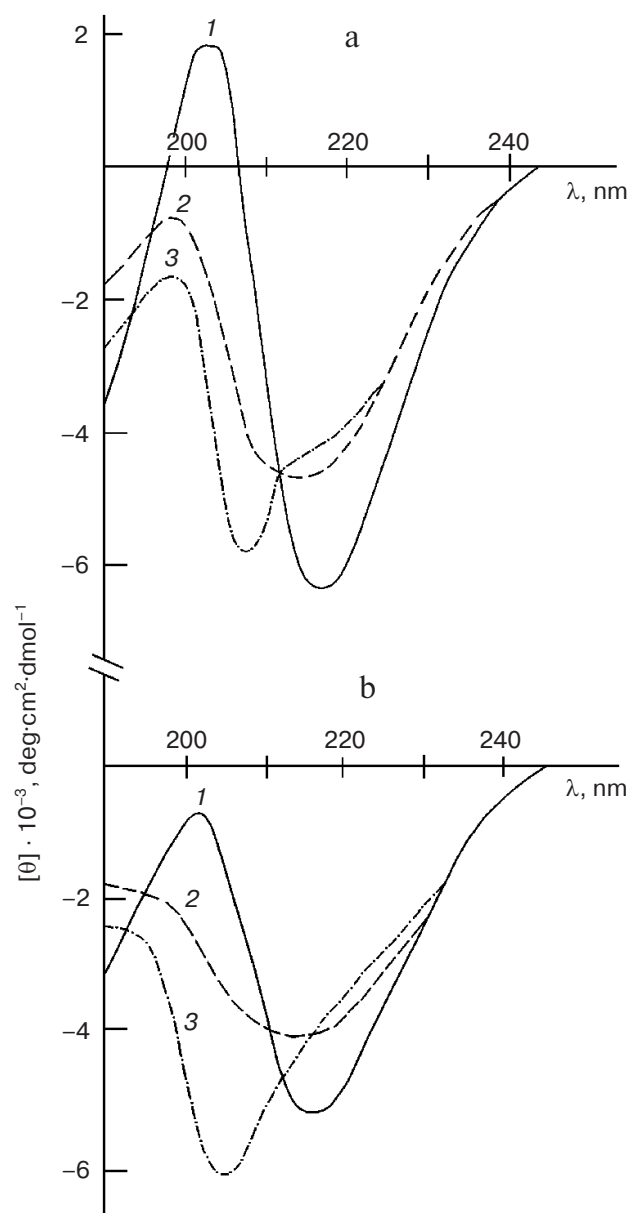


Fig. 4. CD spectra of porins in the far UV region, pH 7.2: a) sample 2 (C-SPh-NA); protein concentration, 150 µg/ml; b) sample 4 (W-SPh-NA/NB); protein concentration, 200 µg/ml. Curves 1, 2, and 3 correspond to $t = 25, 70$, and 85°C , respectively.

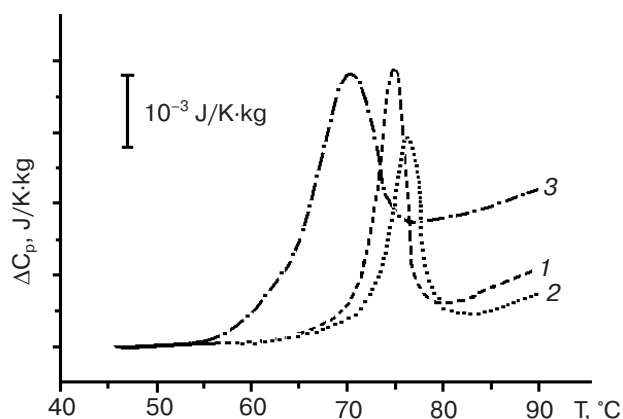


Fig. 5. Temperature dependence of excess specific heat capacity for porin samples: 1) sample 2 (C-SPh-NA); 2) sample 3 (C-SPh-NB); 3) sample 4 (W-SPh-NA/NB). Protein concentration, 0.8–1.3 mg/ml.

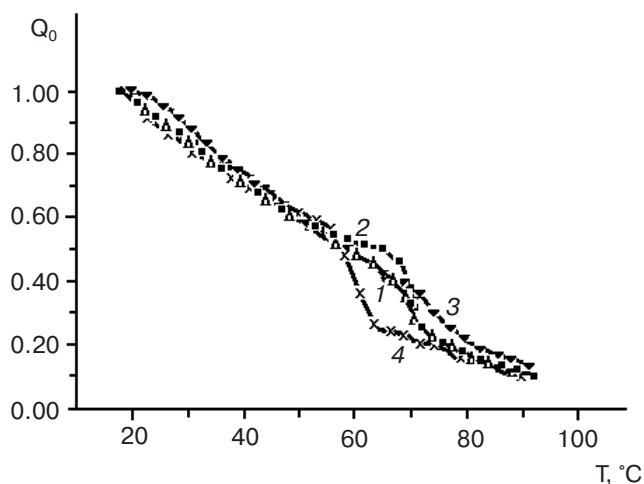


Fig. 6. Dependence of quantum yield of porin fluorescence on temperature: 1) sample 1 (C-LPh-NA); 2) sample 2 (C-SPh-NA); 3) sample 3 (C-SPh-NB); 4) sample 4 (W-SPh-NA/NB). Protein concentration, 70–100 µg/ml.

temperature of the protein by 5–6°C (Table 2) and extends the temperature range of porin melting 2-fold (Fig. 5). It is located in the range of 72–80°C covering 8°C for samples 2 and 3. Porin from the “warm” variant of bacteria melted in the range of 60–75°C covering 15°C.

Intrinsic protein fluorescence. Figure 6 shows the dependence of fluorescence quantum yield of the porin samples on temperature. The thermal transition temperature of these proteins determined from the curves shown is somewhat lower than the corresponding value obtained from microcalorimetry and CD data (Table 3). Based on these values it could be assumed that changes in some domains of the protein leading to alterations in aromatic fluorophores interpositions and accordingly to intensity of fluorescence precede the total melting (registered by

microcalorimetry) and secondary structure changes of the protein molecule. An alternative explanation of the observed differences could be the differences in protein concentration in solutions used for the measurements of protein fluorescence and CD spectra as well as for the melting of porin samples (see figures).

Figure 6 shows that S-shaped part of dependencies of the quantum yield of fluorescence for porins on the temperature is "ended" at the temperature corresponding to the protein melting point. It should be noted that this part of the curve of analyzed dependency is the most pronounced for sample 2, indicating a high degree of cooperativity of thermal transition. In combination the data could be used to estimate the spatial structure of this porin sample isolated from "cold" colonial culture of bacteria during SPh growth phase as the most rigid and ordered on the tertiary and secondary structure level of the protein respectively. The existence of an isodichroic point in CD spectra during the study of the thermodenaturation process of this protein and the smallest deviation of temperature values of thermal transition obtained with different methods indicate sufficiently high level of cooperativity upon conformational changes in the protein during thermodenaturation.

To correlate the changes in spatial organization of the porin molecule on temperature with certain changes in local tertiary protein structure, we analyzed the thermal dependencies of different spectral parameters of the total fluorescence of this porin sample, i.e. quantum yield (Fig. 6) and normalized contributions of different tryptophan classes in protein emission (Fig. 7). These figures show that upon temperature changes the contributions from tyrosine residues and class S tryptophans are virtually unchanged, emission of class I tryptophans is disappearing, and class III tryptophans contribution is grow-

ing. The shape of the curves obtained for porin sample 2 indicates that the largest change in porin structure was observed at 60°C and coincided with the "beginning" of the above-mentioned S-shaped part. The changes in contributions from each class of tryptophans (a_n) in the total protein spectrum can be used to distinguish between the structural transition per se and the baseline monotonous bleaching of porin 2 fluorescence with temperature. This suggests that local tertiary structure changes are connected with an increase in indole fluorophores accessible to water.

The pattern of porin denaturation with temperature we observed is a distinct feature of multidomain proteins, both water-soluble and integral membrane [31]. It is known [32] that having a stable secondary structure the membrane proteins also have a high degree of plasticity on higher levels of molecular organization, which leads to formation of a variety of conformational intermediates upon influence of different denaturing factors.

Pore-forming properties of yersinin in peptidoglycan-protein complexes. Reconstitution of PGPC into lipid bilayer of bacterial membrane is a new approach we developed earlier [13] for investigation of functional properties of *Yersinia* porins using the BLM technique. The advantage of this approach is that porin in complex with peptidoglycan has an environment important for stability and bonds existing in the native membrane. Upon reconstitution in BLM of detergent-solubilized PGPC containing yersinin samples 2-4, discrete fluctuations of current were observed with porin-specific stepped character of change in model membrane conductivity. However, the efficiency of inclusion of complex in the model membrane and the conductivity level of channels formed by complexes in BLM differed significantly.

PGPC containing porin samples 2 and 3 from "cold" *Y. pseudotuberculosis* were highly active. The greatest frequency of inclusion was observed for PGPC containing sample 2. When sample 4 obtained from "warm" bacteria was reconstituted in BLM, the characteristic inclusions were observed only after an increase in complex concentration to the maximum value in the studied concentration range (0.01-2 µg/ml). Because the methods of preparation of both active and inactive complexes were the same, standard conditions of reconstitution in the model membrane were used. The data shown are the result of several experiments, so it is possible to explain the observed discrepancies in pore-formation efficiency in BLM by different functional activity of the studied complexes.

The data provide evidence for significant decrease in porin functional activity upon increase in microorganism growth temperature. The complexes that are inactive in BLM probably contain porins in conformation corresponding to the "closed" state of the pore.

From the analysis of current fluctuations in BLM (Fig. 8) the most probable level of conductivity for active

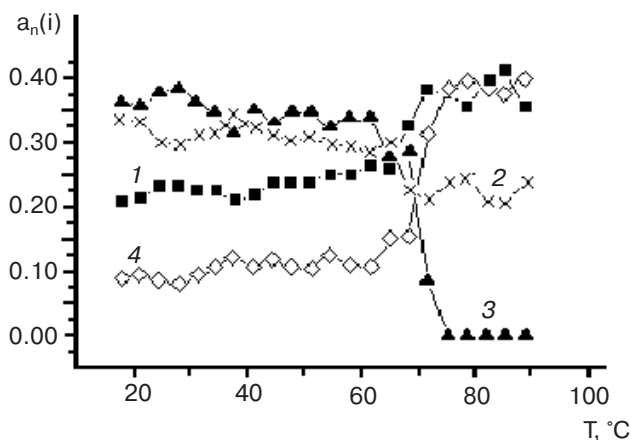


Fig. 7. Changes in normalized contributions of selected tyrosine and tryptophan residues in the protein emission as a function of temperature for sample 2 (C-SPh-NA): 1) tyrosine residues; 2) class S tryptophans; 3) class I tryptophans; 4) class III tryptophans.

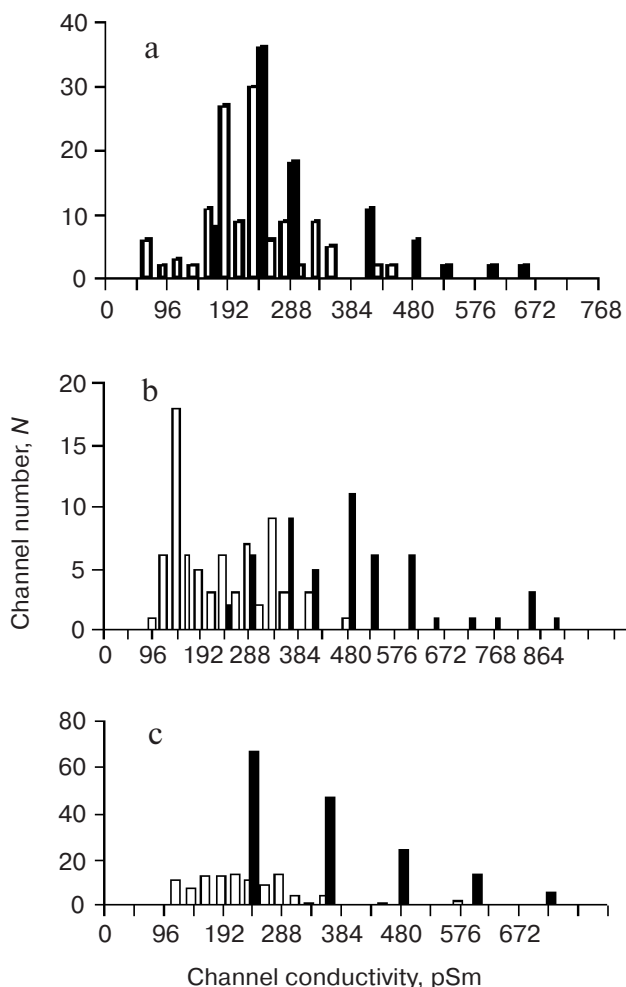


Fig. 8. Conductivity level histogram for pores formed by porin samples in PGPC at membrane potential of 20 mV (filled columns) and 50 mV (empty columns); column width, 24 pSm. *N*, channel number. a) Sample 3 (C-SPh-NB); b) sample 4 (W-SPh-NA/NB); c) sample 2 (C-SPh-NA).

PGPC from “cold” pseudotuberculosis bacteria was equal to 240–300 pSm, while for the complexes from “warm” variant it was 120 pSm. The value of the most probable conductivity induced in BLM for the PGPC samples diminishes in the order $2 \geq 3 \geq 1 \geq 4$. Also, sample 2 forms the most uniform conductivity channels in artificial bilayer as shown in the corresponding figure.

Therefore, *Y. pseudotuberculosis*, similarly to *E. coli*, responds to changes in the environment by changing OM pore size, thus defending the bacterial cell from negative environmental factors. A specific feature of *Y. pseudotuberculosis* is its ability to increase the functional activity of nonspecific porins at low cultivation temperature. We found that medium density and growth phase affect pore-forming properties of porins, and this is correlated with the “order” of the spatial structure of the protein molecules.

The results provide data on the dependence of spatial organization and functional activity of OmpF-like porin

from pseudotuberculosis OM on the cultivation conditions. This work therefore provides experimental support for the existing opinion about high degree of conformational and functional plasticity of nonspecific porins from gram-negative bacteria during their adaptation to the changes in the environment. Optical and pore-forming properties of the porin isolated from “warm” *Y. pseudotuberculosis* indicated that the protein less stable to temperature with low functional activity (smaller pore diameter) was expressed under these conditions. These results are in good agreement with published data indicating that nonspecific porin biosynthesis switches from OmpF to OmpC proteins [5] at elevated temperatures. Hence *Yersinia* porins do not differ from the similar proteins of other gram-negative bacteria.

We demonstrated the correlation between elevated LPE content in “cold” colonial culture of *Y. pseudotuberculosis* (i.e. conditions closest to natural) and spatial structure features of porin isolated from it. This protein had the most compact spatial structure and the highest pore-forming activity. LPE is known as a molecular chaperon of integral membrane proteins. It defends them from heat shock by preventing aggregation and favoring the formation of functionally active protein [33, 34]. The anomalously high LPE content in the saprophyte *Yersinia* might thus provide an instrument supporting stable conformation of porins and increasing its adaptation abilities.

This work was performed with financial support from the Russian Academy of Sciences Presidium program “Molecular and cellular biology”.

REFERENCES

1. Marsh, D. (1993) in *New Comprehensive Biochemistry* (Watts, A., ed.) Elsevier, Amsterdam, pp. 41–66.
2. Selinsky, B. S. (1992) in *Structure of Biological Membranes* (Yeagle, P., ed.) CRC Press, Boca Raton, FL, pp. 603–651.
3. Wang, X., Bogdanov, M., and Dowhan, W. (2002) *EMBO J.*, **21**, 5673–5681.
4. De Cock, H., Pasveer, M., Tomassen, J., and Bouveret, E. (2001) *Eur. J. Biochem.*, **268**, 865–875.
5. Delcour, A. (1997) *FEMS Microbiol. Lett.*, **151**, 115–123.
6. Buehler, L. K., Kusumoto, S., Zhang, H., and Rosenbusch, J. P. (1991) *J. Biol. Chem.*, **266**, 24446–24450.
7. Panikov, N. S. (1991) in *Kinetics of Bacterial Growth* (Zvyagintsev, D. G., ed.) [in Russian], Nauka, Moscow, pp. 211–221.
8. Brubacker, R. R. (1991) *Clin. Microbiol. Rev.*, **4**, 309–324.
9. Straley, S. C., and Perry, R. (1995) *Trends Microbiol.*, **3**, 310–317.
10. Bengoechea, J. A., Dfas, R., and Moriyon, I. (1995) *Infect. Immun.*, **64**, 4891–4899.
11. Bengoechea, J. A., Brandenburg, K., Seydel, U., Dfas, R., and Moriyon, I. (1998) *Microbiology*, **144**, 1517–1526.

12. Baholdina, S. I., Krasikova, I. N., Shubin, F. N., Busoleva, L. S., and Solov'eva, T. F. (2001) *Biochemistry (Moscow)*, **66**, 415-421.
13. Vostrikova, O. P., Lihatskaya, G. N., Novikova, O. D., and Solov'eva, T. F. (2000) *Biol. Membr. (Moscow)*, **17**, 399-409.
14. Schnaitman, C. A. (1970) *J. Bacteriol.*, **104**, 890-901.
15. Nurminen, M. (1985) in *Methods for Molecular Characterization* (Korhonen, N. K., ed.) Elsevier Science Publishers, N. Y., pp. 293-300.
16. Novikova, O. D., Fedoreeva, L. I., Khomenko, V. A., Portnyagina, O. Yu., Ermak, I. M., Lihatskaya, G. N., Moroz, S. V., Solov'eva, T. F., and Ovodov, Yu. S. (1993) *Bioorg. Khim.*, **19**, 536-547.
17. Laemmli, U. K. (1970) *Nature*, **227**, 680-685.
18. Gal, E., Medyeshi, G., and Verezkei, L. (1982) *Electrophoresis in Macromolecules Separation* [Russian translation], Mir, Moscow, p. 157.
19. Tsai, C. M., and Frash, C. E. (1982) *Analyt. Biochem.*, **119**, 115-119.
20. Dubois, M., Gilles, K. A., Hamilton, J. K., et al. (1956) *Analyt. Chem.*, **28**, 350-356.
21. Markwel, M. A. K., Haas, S. M., Bieber, L. L., and Tolbert, N. E. (1978) *Analyt. Biochem.*, **87**, 206-210.
22. Provencher, C. W., and Glocker, J. (1981) *Biochemistry*, **20**, 34-37.
23. Emelyanenko, V. I. (1991) *GPS*, **55**, 587-593.
24. Burstein, T. A., Vedenkina, N. S., and Ivkova, M. N. (1973) *Photochem. Photobiol.*, **18**, 263-279.
25. Marquardt, D. W. (1963) *J. Soc. Indust. Appl. Math.*, **11**, 431-441.
26. Lihatskaya, G. N., Novikova, O. D., Solov'eva, T. F., and Ovodov, Yu. S. (1985) *Biol. Membr. (Moscow)*, **2**, 1219-1224.
27. Chehin, R., Iloro, I., Marcos, M. J., Villar, E., Shnyrov, V. L., and Arrondo, J. L. R. (1999) *Biochemistry*, **38**, 1525-1530.
28. Kazlauskaitė, J., Young, A., Gardner, C. E., Macpherson, J. V., Venieb-Brayan, C., and Pinheiro, T. J. (2005) *Biochem. Biophys. Res. Commun.*, **328**, 292-305.
29. Ven'yaminov, S. Yu., Kosih, V. G., Kholodkov, O. A., and Bur'yanov, Ya. I. (1990) *Bioorg. Khim.*, **16**, 47-51.
30. France, L. L., Kieleczawa, J. J., Dunn, J. J., Hind, G., and Sutherland, J. C. (1992) *Biochim. Biophys. Acta*, **1120**, 59-68.
31. Damaschun, G., Damaschun, H., Gast, K., and Zirwer, D. (1998) *Biochemistry (Moscow)*, **63**, 259-275.
32. Pfeil, W. (1998) *Biochemistry (Moscow)*, **63**, 294-302.
33. Bogdanov, M., Umeda, M., and Dowhan, W. (1999) *J. Biol. Chem.*, **274**, 12339-12345.
34. Kern, R., Joseleau-Petit, D., Chattopadtyay, K., and Richarme, G. (2001) *Biochem. Biophys. Res. Commun.*, **289**, 1268-1274.